



Contents lists available at ScienceDirect

# Journal of Quantitative Spectroscopy & Radiative Transfer

journal homepage: [www.elsevier.com/locate/jqsrt](http://www.elsevier.com/locate/jqsrt)

## Updated database plus software for line-mixing in CO<sub>2</sub> infrared spectra and their test using laboratory spectra in the 1.5–2.3 μm region

J. Lamouroux<sup>a</sup>, H. Tran<sup>b</sup>, A.L. Laraia<sup>a</sup>, R.R. Gamache<sup>a</sup>, L.S. Rothman<sup>c</sup>,  
I.E. Gordon<sup>c</sup>, J.-M. Hartmann<sup>b,\*</sup>

<sup>a</sup> University of Massachusetts School of Marine Sciences, Department of Environmental, Earth, and Atmospheric Sciences, One University Avenue, University of Massachusetts Lowell, Lowell, MA 01854-5045, USA

<sup>b</sup> Laboratoire Interuniversitaire des Systèmes Atmosphériques (LISA), CNRS (UMR 7583), Universités Paris XII et Paris VII, 94010 Créteil, Cedex, France

<sup>c</sup> Harvard-Smithsonian Center for Astrophysics, Atomic and Molecular Physics Division, Cambridge, MA 02138-1516, USA

### ARTICLE INFO

#### Article history:

Received 9 February 2010

Received in revised form

9 March 2010

Accepted 9 March 2010

#### Keywords:

CO<sub>2</sub>

Line mixing

Infrared spectra

Remote sensing

### ABSTRACT

In a previous series of papers, a model for the calculation of CO<sub>2</sub>-air absorption coefficients taking line-mixing into account and the corresponding database/software package were described and widely tested. In this study, we present an update of this package, based on the 2008 version of HITRAN, the latest currently available. The spectroscopic data for the seven most-abundant isotopologues are taken from HITRAN. When the HITRAN data are not complete up to  $J'' = 70$ , the data files are augmented with spectroscopic parameters from the CDS-296 database and the high-temperature CDS-1000 if necessary. Previously missing spectroscopic parameters, the air-induced pressure shifts and CO<sub>2</sub> line broadening coefficients with H<sub>2</sub>O, have been added. The quality of this new database is demonstrated by comparisons of calculated absorptions and measurements using CO<sub>2</sub> high-pressure laboratory spectra in the 1.5–2.3 μm region. The influence of the imperfections and inaccuracies of the spectroscopic parameters from the 2000 version of HITRAN is clearly shown as a big improvement of the residuals is observed by using the new database. The very good agreements between calculated and measured absorption coefficients confirm the necessity of the update presented here and further demonstrate the importance of line-mixing effects, especially for the high pressures investigated here. The application of the updated database/software package to atmospheric spectra should result in an increased accuracy in the retrieval of CO<sub>2</sub> atmospheric amounts. This opens improved perspectives for the space-borne detection of carbon dioxide sources and sinks.

© 2010 Elsevier Ltd. All rights reserved.

### 1. Introduction

Taking line-mixing among CO<sub>2</sub> lines into account is often unavoidable for accurate treatments of atmospheric spectra. This may lead to significant improvements in the agreement between measured and calculated spectra with positive consequences for various types of retrievals

(trace species amounts, temperature and pressure profiles, CO<sub>2</sub> atmospheric amount, see Sec. VII.4 of Ref. [1]). For such remote-sensing purposes, a line-mixing model was developed more than five years ago [2,3] from which a database and Fortran programs were built for atmospheric spectra calculations [4]. The improvements brought by these tools have been widely demonstrated, recent examples being given in Refs. [5,6] for temperature and CO<sub>2</sub> concentration retrievals, respectively. Nevertheless, the database/software package of Ref. [4] has limitations and imperfections due to the fact that its

\* Corresponding author. Tel.: +33 145176542.

E-mail address: hartmann@lisa.univ-paris12.fr (J.-M. Hartmann).

spectroscopic files were built from the 2000 edition of the HITRAN database [7] (state-of-the-art at the time the package was built). These defects, which affect the quality of spectra predictions, are, among other problems, the lack of data for many weak bands, inaccurate line intensities (an approximate 10% overestimation of those of the  $(2\nu_1+\nu_3)_{III}$  band, for instance) and the absence of values for the air-induced pressure shifts and broadening coefficients by  $H_2O$ . In the last decade, significant progress has been made, particularly in the regions near 1.6 and 2.1  $\mu m$  which are used for the retrieval of  $CO_2$  atmospheric amounts (see Refs. [6,8] and references therein). In fact, the Orbiting Carbon Observatory project (OCO [9], unfortunately lost due to a launch failure but whose replacement is under study by NASA) and the Greenhouse Gases Observatory Satellite (GOSAT [10]) have put very high constraints [11] on the quality of the spectroscopic data. This has stimulated numerous high-quality laboratory studies such as those whose results are reviewed in Ref. [12], leading, in 2009, to a significant update [13] of the HITRAN database. In addition, recent advances have been made in the knowledge of the air-induced line-shifts [14] and of the broadening coefficients due to collisions with  $H_2O$  [15]. This progress, the needs for very accurate  $CO_2$  spectra predictions for remote sensing and promising results obtained for atmospheric  $CO_2$  retrievals [6] call for an update of the package of Ref. [4]. This is the subject of the present paper where tests are also made, for the first time in the 1.5–2.3  $\mu m$  region used for the monitoring of atmospheric  $CO_2$ , using high-pressure laboratory spectra.

## 2. Line-mixing database and software

Since the former versions of the  $CO_2$  line-mixing database and software have been presented in detail in Refs. [3,4], only the changes and improvements are described below. Nevertheless, recall that the spectroscopic parameters in the package of Ref. [4] were extracted from the 2000 version of the HITRAN database [7] and that the line-mixing parameters were constructed using the model presented in Refs. [2,3].

The new version of the line-mixing database has essentially the same structure as the former one. It includes relaxation matrix files for each type of band (defined by the values of the vibrational angular momentum  $\ell_2$  in the lower and upper vibrational states), spectroscopic files for each band of each isotopologue, and a file giving overall information on the bands.

The relaxation matrix files have been left unchanged in the absence of any demonstration for the need of an improved line-mixing model. Note that this quality is confirmed by the comparisons between measured and calculated spectra presented in Section 4.

For the spectroscopic files, their names have been changed to account for the HITRAN database choice, made in 2004 [16], to switch from vibrational level index numbering to explicit vibrational quantum numbers. For the  $(\nu'_1\nu'_2\ell'\nu'_3)_{i'} \leftarrow (\nu''_1\nu''_2\ell''\nu''_3)_{i''}$  band of the  $CO_2$  isotopologue number  $i$ , the file name is then  $Siv'_1\nu'_2\ell'\nu'_3n'v''_1\nu''_2\ell''\nu''_3n''XY.dat$ , where each variable is

a single character. The last characters, X and Y, are used to split bands of asymmetric isotopologues involving both odd and even  $J$  rotational levels into two uncoupled sub-bands, as done previously [4,17]. The default value of XY is “ ” (blanks) except in the above-mentioned case where it takes the values “I” and “II” for the two sub-bands. For instance, for the  $(\nu_1-\nu_2)$  band (i.e.  $10^0O_2 \leftarrow 01^1O_1$ ) of  $^{12}C^{16}O_2$ , the file name changes from S1003002.dat to S11000201101.dat. The files themselves have been updated and completed as follows.

Most of the line positions, intensities, identifications and lower-state energies have been taken from the 2008 version of the HITRAN database [13]. As shown below, this leads to significant changes and improvements, in particular for the  $2\nu_1+\nu_3$  triad and  $3\nu_1+\nu_3$  tetrad. As mentioned previously [4,18], overly severe truncations of the relaxation matrices must be avoided for a correct treatment of line-mixing effects. For atmospheric temperatures, this imposes to have data for lines with initial quantum number up to a (conservative) minimum of about 70. For bands for which the HITRAN data do not match this criterion, additional spectroscopic data were taken, when possible, from the CDS-296 [19] database and, if CDS-296 does not have the needed transitions, from the CDS-1000 [20] database. To simplify this procedure, these databases were converted to the HITRAN format, including the conversion of the transition moment squared to the Einstein A-coefficients, and all data to a reference temperature of 296 K. Note that great care was taken to check for the consistency, in frequency and intensity, of all these data sources and that it was found that differences between common data in the three databases are small. This procedure of data assembly still leaves a number of (very weak) bands incomplete. In this case, the software for the calculation of absorption coefficients uses Voigt line shapes, thus neglecting line-mixing effects. This is likely of completely negligible consequences for atmospheric spectra calculations due to the weakness of the concerned bands.

Because of inconsistencies in the air-broadened half-widths for various lines and bands (especially for  $J > 50$ ) in HITRAN 2008, the air-broadening half-widths and their temperature dependences were replaced in all the bands by a coherent set of values. The latter were obtained, for  $^{12}C^{16}O_2$ , using the empirical polynomial expression derived in Ref. [21]. This neglects band-to-band variations of the width, a good approximation based on the weak dependence of the intermolecular potential and which has, to our knowledge, never been proved insufficient. Nevertheless, in the future the polynomial expressions from Ref. [21] will need to be replaced by new ones, which will be derived based on the fit to the newest experimental data, especially for  $J > 50$ .  $CO_2$  line broadening coefficients (and their temperature exponents) induced by collisions with  $H_2O$ , not present in the former version of our database [4], have also been added. They are again assumed independent of the band and were constructed using the data of Ref. [15]. Note that for high-accuracy retrievals from  $CO_2$  absorption in a humid atmosphere, accounting for this broadening contribution is necessary since the broadening coefficients of  $CO_2$  lines by  $H_2O$  are

typically twice greater than those by air. In fact, for 2% water in air (about 100% humidity at 1 atm and 293 K), the line widths are then about 2% greater than in dry air, a difference that cannot be neglected for high-accuracy CO<sub>2</sub> retrievals. Finally, in order to (at least approximately) take into account the isotopologue mass dependence of the line broadenings for the different isotopologues, Eq. (A4) of the Appendix was applied.

Finally the air-induced pressure shifts (assumed temperature independent in the absence of such information), not given for the majority of transitions in HITRAN2008, were added. Their values were generated, for each line of each band, using the empirically derived procedure described in Ref. [14].

The file giving general information on the bands still provides the band identification, its overall integrated intensity, and the minimum and maximum wavenumbers in which the band contribution will be computed. These two limits were determined, in a very conservative way, by considering the most absorbing terrestrial atmospheric path possible and choosing a cut-off of the total absorbance of 10<sup>-4</sup>.

Note that, as a result of the progress since the 2000 edition of HITRAN, the numbers of bands and data are significantly larger in the new version of our database than in the former one. For instance, there are now about 3600 bands (or sub-bands) where previously there were only about 600. As a result, computations may be significantly lengthier than before. A cut-off criterion on the total band intensity can be used to limit the number of retained bands (through an input parameter to the “DetBand” subroutine) but we leave the choice of its value to the user. The construction of look up tables is likely a good way to avoid lengthy on-the-fly calculations.

Only slight modifications to the *Fortran* software have been made. These take into account the change of the names of the spectroscopic files and the added data (shifts and H<sub>2</sub>O broadening). Note that, since the broadening of CO<sub>2</sub> lines by H<sub>2</sub>O is now taken into account, users must provide the water vapor mole fraction (in addition to the temperature, pressure, CO<sub>2</sub> mole fraction and spectral range) for calculations of absorption coefficients.

### 3. Laboratory experiments and band intensities

#### 3.1. Experiments

Transmission spectra of pure CO<sub>2</sub> and CO<sub>2</sub>-N<sub>2</sub> mixtures have been recorded with the experimental set-up used for previous similar studies at LISA in Créteil. The apparatus uses a Tungsten halogen lamp, a Bruker IFS 66 V Fourier transform spectrometer with a CaF<sub>2</sub> beam splitter, a L=215 cm long coolable single pass cell, that can withstand pressures up to 150 atm, and an InSb detector. In the present experiments, the spectral resolution of 1 cm<sup>-1</sup> was used and spectra were recorded from 2500 to 8000 cm<sup>-1</sup> by accumulating 512 scans. For low-temperature studies, the cell was first cooled through circulation of liquid nitrogen down to a temperature of about 200 K

measured by several type-K thermocouples. The liquid nitrogen flow was then stopped and after the temperature reached the desired value the spectra were recorded. Thanks to the high thermal inertia of the cell, the temperature did not vary by more than 1 K during the acquisition of one spectrum (about 10 min).

The experiment was carried out as follows: A spectrum was first recorded with an empty cell, providing the 100% transmission reference. Carbon dioxide was then introduced into the cell before nitrogen was added (in the case of studies devoted to mixtures). For pure CO<sub>2</sub> measurements at room temperature, the initial pressure used was about 45 atm. For CO<sub>2</sub>-N<sub>2</sub> mixtures, a suitable quantity of CO<sub>2</sub> was first introduced (such that the minimum transmission at the peak of the bands under study did not saturate, e.g. typically 0.6 and 6 atm for the 4900 and 6200 cm<sup>-1</sup> region at room temperature, respectively) before N<sub>2</sub> was added up to a total pressure of about 70 atm. The cell was then closed and the mixture was left overnight to homogenise. A series of spectra was recorded the next day, starting from the initial (highest) total pressure and progressively emptying the cell (by steps of typically 5 or 10 atm). After the lowest pressure (typically 10 atm) spectrum was recorded, the cell was emptied and a second reference spectrum was acquired. Transmissions are obtained from the ratio of recordings obtained with a gas sample and the empty cell (the latter being multiplied by an ad-hoc constant to obtain unity transmissions in the transparency regions). In these experiments, high purity CO<sub>2</sub> and N<sub>2</sub> gases have been used and pressures were measured by various gauges (0–1.5, 0–25 and 0–400 atm) with an accuracy better than 1%. The densities of molecules were deduced for the pressure and temperature readings using PVT data [22]. Note that using densities and not pressures is particularly important for high-pressure CO<sub>2</sub>, which shows large deviations from the perfect gas law.

#### 3.2. Allowed band intensities

The first tests of our measurements have been made by considering three spectral regions (Table 1), which contain CO<sub>2</sub> (allowed) electric dipole bands but show no evidence for any Collision Induced Absorption (CIA) processes. We have retained spectra recorded under sample conditions for which measured transmissions do not saturate (e.g. Fig. 1). With the cell (length) and pressures used in this study, pure CO<sub>2</sub> recordings have been used for the region between 5950 and 6610 cm<sup>-1</sup> (3ν<sub>1</sub>+ν<sub>3</sub> tetrad) whereas diluted (in N<sub>2</sub>) samples have been used for the 4740–5200 cm<sup>-1</sup> (2ν<sub>1</sub>+ν<sub>3</sub> triad) and 6830–7040 cm<sup>-1</sup> (3ν<sub>3</sub> band) intervals. Typical transmissions τ(σ) are displayed in Fig. 1 for the first region. From such data, the associated absorption coefficients α(σ)=ln[1/τ(σ)]/L (in cm<sup>-1</sup>) are then calculated and their area A(σ<sub>Min</sub>, σ<sub>Max</sub>) (in cm<sup>-2</sup>) are obtained by spectral integration between σ<sub>Min</sub> and σ<sub>Max</sub> (on each side of absorption features, where absorption is negligible). Measured values of A(5950,6610) at room temperature are plotted in Fig. 2. They show a very nice linearity with

**Table 1**

Values of the integrated intensities ( $\text{cm}^{-2}/\text{atm}$ ) of allowed  $\text{CO}_2$  bands in various spectral regions at 295.15 K. The numbers between parentheses in column 3 are the RMS of the various measured values.

$\sigma_{\text{Min}} - \sigma_{\text{Max}}$ ( $\text{cm}^{-1}$ )	#Meas	$S^0$ (present work) ( $\text{cm}^{-2}/\text{atm}$ )	$S^0$ from Refs. [12,13] ( $\text{cm}^{-2}/\text{atm}$ )	% Diff.
4740–5200	6	1.39370 (0.00008)	1.40960	1.1
5950–6610	9	0.02722 (0.00002)	0.02732	0.4
6830–7040	6	0.04130 (0.00007)	0.04207	1.8

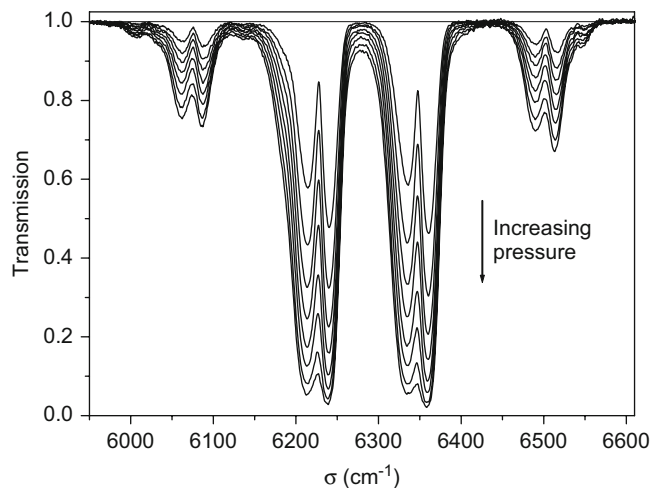


**Fig. 1.** Measured transmission spectra (215 cm long path) for pure  $\text{CO}_2$  at 295.2 K and seven pressures from about 10 atm to about 45 atm by steps of about 5 atm.

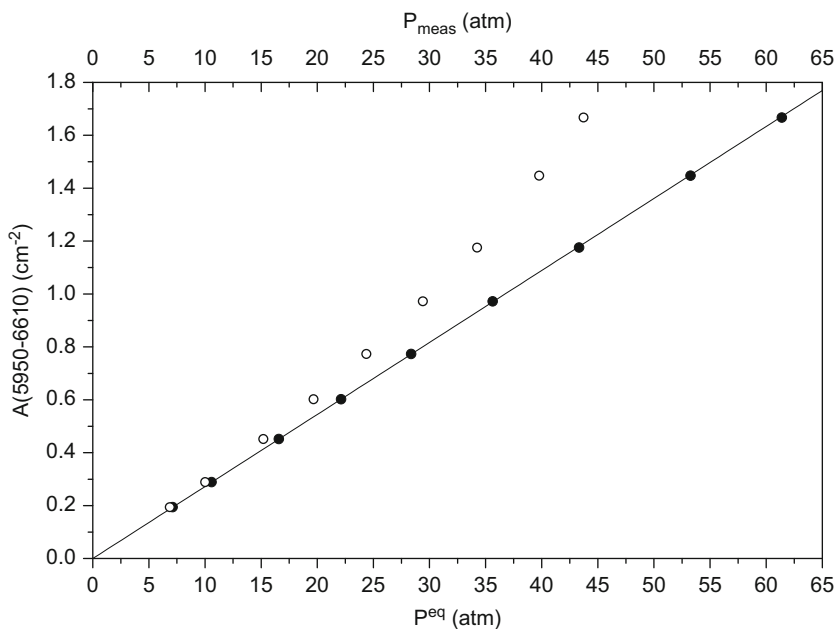


**Fig. 2.** Integrated intensity (area) between  $5950$  and  $6610 \text{ cm}^{-1}$ , obtained from pure  $\text{CO}_2$  measurements (Fig. 1) at 295.2 K, plotted vs the measured pressure  $P_{\text{meas}}$  ( $\circ$ , top x-axis) and the equivalent pressure  $P^{\text{eq}}$  ( $\bullet$ , bottom x-axis). The line corresponds to the law  $S(5950,6610) = 0.02722 \times P^{\text{eq}}$ .

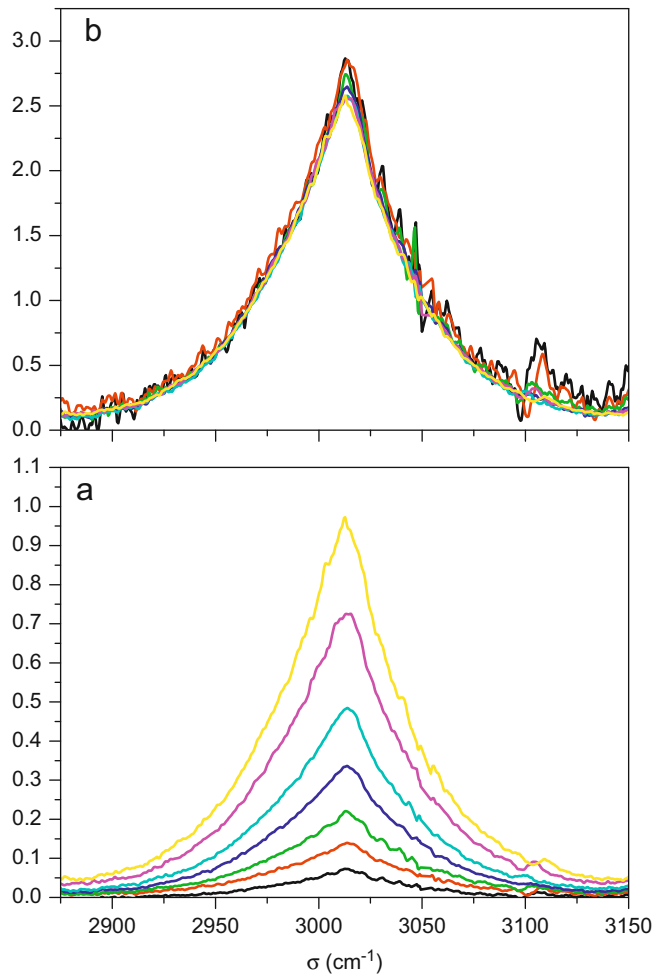


**Fig. 3.** Measured absorption coefficients (bottom) and associated square density normalized values (top) for pure CO<sub>2</sub> at 295.15 K and seven total pressures from 15 to 44 atm: (b) Dens normalized Abs ( $10^{-6} \text{ cm}^{-1}/\text{atm}^2$ ) and (a) Abs Coeff ( $10^{-2} \text{ cm}^{-1}$ ).

**Table 2**

Values of the integrated intensities  $S^{\text{CIA}}$  ( $\text{cm}^{-2}/\text{atm}^2$ ) and peak absorption  $peak^{\text{CIA}}$  ( $\text{cm}^{-1}/\text{atm}^2$ ) for collision induced absorption in various spectral regions at 295.15 K. Results are for CO<sub>2</sub> in N<sub>2</sub>, except for the first region where pure CO<sub>2</sub> measurements have been used.

$\sigma_{\text{Min}} - \sigma_{\text{Max}}$ ( $\text{cm}^{-1}$ )	#Meas	$S^{\text{CIA}}$ and $peak^{\text{CIA}}$ (present work) ( $\text{cm}^{-2}/\text{atm}^2$ and $\text{cm}^{-1}/\text{atm}^2$ )	$S^{\text{CIA}}$ and $peak^{\text{CIA}}$ (previous studies) ( $\text{cm}^{-2}/\text{atm}^2$ and $\text{cm}^{-1}/\text{atm}^2$ )
2850–3150	9	$2.4 \times 10^{-4}$ and $2.7 \times 10^{-6}$	$2.7 \times 10^{-4}$ and $\approx 3 \times 10^{-6}$ [23]
4500–4735	6	$9.1 \times 10^{-5}$ and $1.3 \times 10^{-6}$	$1.02 \times 10^{-4}$ and $1.44 \times 10^{-6}$ [24]
4740–5200	6	$< 10^{-4}$ and $< 10^{-6}$	
5950–6610	9	$< 3 \times 10^{-6}$ and $< 3 \times 10^{-8}$	
6830–7040	6	$< 5 \times 10^{-6}$ and $< 5 \times 10^{-8}$	

the equivalent pressure  $P^{\text{eq}}(P_{\text{meas}}, T)$ <sup>1</sup> which is not the case when the measured pressure is used, due to the large deviations from the perfect gas law for CO<sub>2</sub> at elevated densities. Linear fits, vs the CO<sub>2</sub> amount in the mixture, of

the areas obtained in the three spectral regions studied give the (CO<sub>2</sub>-density normalized) integrated intensities (i.e.  $S^0(\sigma_{\text{Min}}, \sigma_{\text{Max}}) = A(\sigma_{\text{Min}}, \sigma_{\text{Max}})/P_{\text{CO}_2}^{\text{eq}}$ , in  $\text{cm}^{-2}/\text{atm}$ ). The results obtained at room temperature are summarized in Table 1 where they can be compared with those obtained from the HITRAN 2008 database [13] (these particular data originate from Ref. [12]). As can be seen, the agreement is excellent, showing the consistency and accuracy of our experiments.

<sup>1</sup> For convenience we use the “equivalent pressure  $P^{\text{eq}}$  such that the density of a perfect gas at pressure  $P^{\text{eq}}$  and temperature  $T$  is the same as that of the experiment.

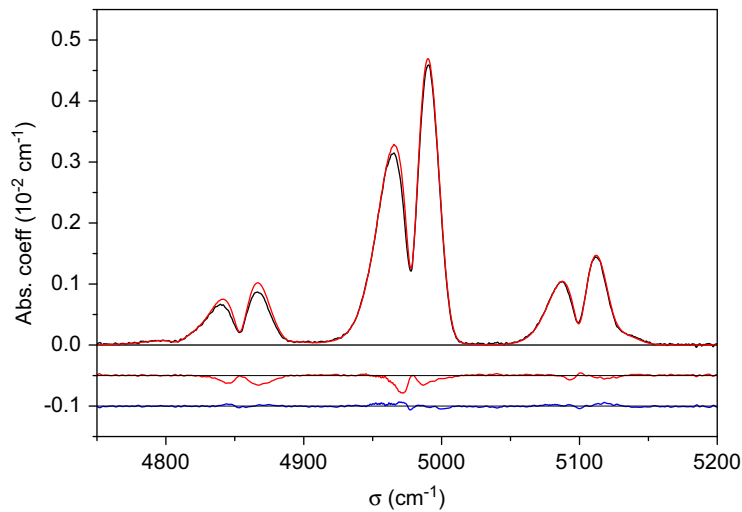


**Fig. 4.** Measured (—) and calculated (—, with the former version of our database and software) absorption coefficients for 1% CO<sub>2</sub> in 18.3 atm of N<sub>2</sub> at 295.15 K in the region of the  $2\nu_1 + \nu_3$  triad. The lower traces give the shifted meas-calc residuals obtained with the former (—) and new (—) version of our database and software.

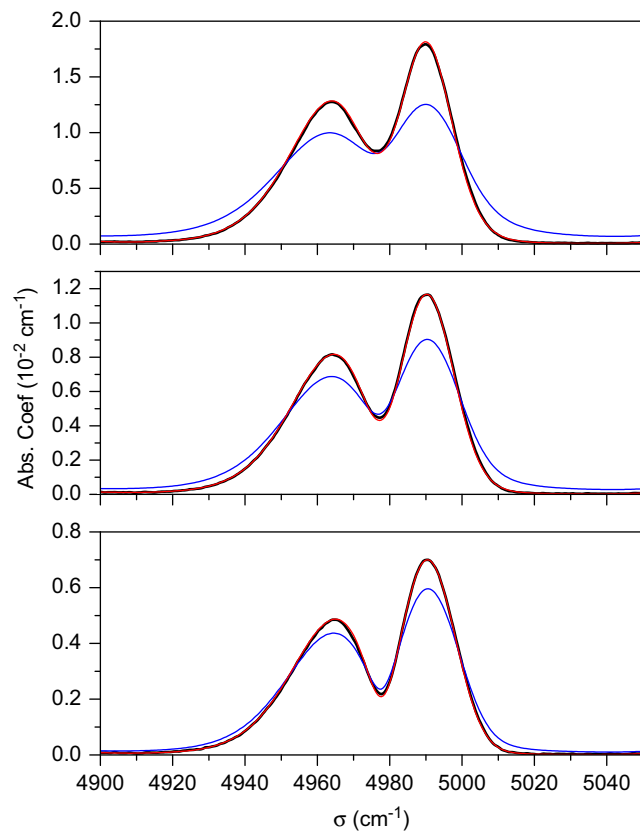


**Fig. 5.** Absorption coefficients for 1% CO<sub>2</sub> in various pressures (from bottom to top: 28.1, 47.6, and 76.0 atm) of N<sub>2</sub> at 295.15 K in the region of the  $(2\nu_1 + \nu_3)_2$  band. — are measured values, whereas — and — have been calculated with the old and new version of our database and software, respectively, neglecting line-mixing and taking this process into account.

### 3.3. Collision Induced Absorption (CIA) intensities

#### 3.3.1. “Obvious” bands

From previous studies [23,24] and examination of the spectra, two collision induced absorption features have been unambiguously identified, centered near 3010 and 4680  $\text{cm}^{-1}$ . The first, recorded with pure  $\text{CO}_2$  for measured pressures between 10 and 43 atm is displayed in Fig. 3 showing (Fig. 3b) that absorption is, as expected for a pure CIA process, proportional to the squared  $\text{CO}_2$  density. The second CIA feature, which we measured for  $\text{CO}_2+\text{N}_2$  mixtures, is a double transition near 4680  $\text{cm}^{-1}$ . For these two CIA bands, the integrated intensities and peak absorption values are given in Table 2 where they can be (successfully) compared with previous determinations.

#### 3.3.2. “Hidden” bands?

The question of (weak) CIA “hidden” below the (strong) allowed dipole bands, as observed in the  $\text{O}_2$  A-band region [25] is still open at this step. Indeed, as exemplified by Fig. 2, the integrated intensities obtained from the measurements in the allowed bands show remarkably linear behaviors vs the  $\text{CO}_2$  density indicating that CIA contributions are small. In order to go further, we have carefully examined the upper bound value for this

process. We thus write, as in Ref. [25]

$$\frac{A^{\text{Meas}}(P_{\text{CO}_2}, P_{\text{Tot}}, \sigma_{\text{Min}}, \sigma_{\text{Max}})}{P_{\text{CO}_2}^{\text{eq}}} = S^0(\sigma_{\text{Min}}, \sigma_{\text{Max}}) + P_{\text{Tot}}^{\text{eq}} S^{\text{CIA}}(\sigma_{\text{Min}}, \sigma_{\text{Max}}), \quad (1)$$

where  $S^{\text{CIA}}$  (in  $\text{cm}^{-2}/\text{atm}^2$ ) is the (eventual) density normalized integrated intensity due to CIA in the considered region,  $S^0$  (cf. Section 3.2) being the value associated with the allowed dipole. From the scatter of values of the first term in Eq. (1) obtained from our measurements, upper limits for  $S^{\text{CIA}}$  have been determined, which are reported in Table 2. In order to evaluate the consequences for atmospheric spectra, one must know the peak absorption. Assuming that all CIA bands have the same shape, the measured values in Table 2 show that the maximum absorption (in  $\text{cm}^{-1}/\text{atm}^2$ ) is about 1% of the integrated intensity (in  $\text{cm}^{-2}/\text{atm}^2$ ). Hence, for all regions in Table 2, the density normalized CIA peak absorption is lower than a few  $10^{-6} \text{cm}^{-1}/\text{atm}^2$ . Assuming that the peak absorption (in  $\text{cm}^{-1}/\text{amagat}^{-2}$ ) is independent on temperature, the overall atmospheric absorbance has been calculated for a standard atmosphere. The value obtained is lower than a few  $10^{-4}$  for an air mass of 1. Hence, even for large airmasses, CIA would make a contribution to atmospheric spectra below a fraction of a percent.

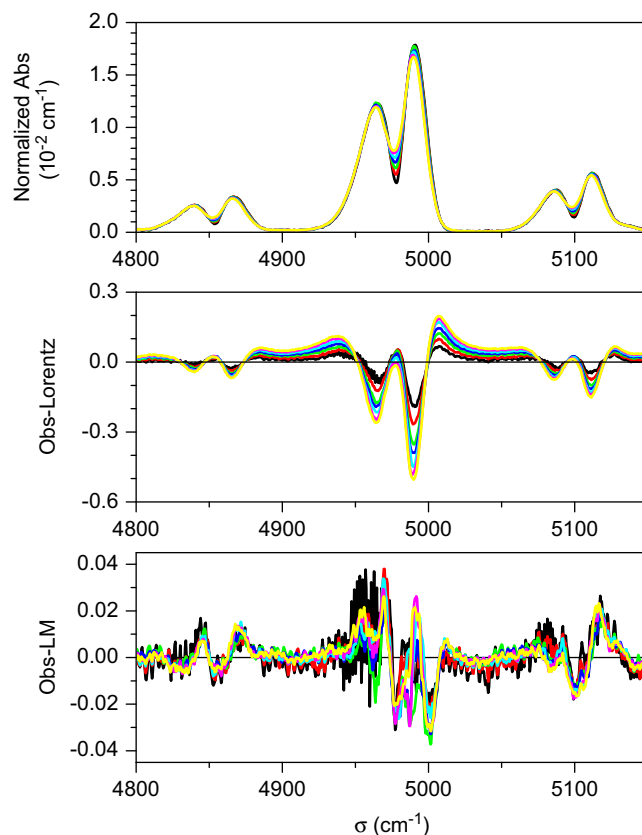


**Fig. 6.** Absorption coefficients and meas-calc residuals for 1%  $\text{CO}_2$  in seven pressures (from 19 to 76.0 atm) of  $\text{N}_2$  at 295.15 K in the region of the  $(2\nu_1+\nu_3)$  triad. The top panel displays the measured absorptions normalized to unity area through integration over  $\sigma$ . The middle and lower panels display the residuals (meas-calc) obtained from calculations with our new database, respectively, neglecting line-mixing and taking this process into account.

#### 4. Comparisons between measured and calculated spectra

Before presenting comparisons between measured and calculated spectra let us mention four points: (i) First is that calculations are made with the full relaxation matrix  $W$  according to Eq. (2) of Ref. [2], for instance. This is made taking into account the off-diagonal elements or, when line-mixing is neglected, only the diagonal ones (i.e. the line broadening and shifting coefficients, thus leading to Lorentzian line shapes). Note that no element of the real part of the relaxation matrices was adjusted. (ii) The measured spectra are for  $\text{CO}_2+\text{N}_2$  mixtures while the database is for  $\text{CO}_2$  highly diluted in air. To correct for this difference, the off-diagonal elements of  $W$  have been multiplied by a constant factor equal to  $\langle \gamma(P_{\text{CO}_2}, P_{\text{N}_2}, T) / (P_{\text{CO}_2} + P_{\text{N}_2}) \rangle / \langle \gamma_{\text{CO}_2\text{-air}}^0(T) \rangle$ , where  $\langle \dots \rangle$  denotes an intensity weighted average. (iii) Also note that, in the studied regions, the most intense bands are all of  $\Sigma-\Sigma$  symmetry and the vibrational angular momenta of their lower and upper states is zero. Hence, all these bands were computed with the same relaxation matrix. (iv) Finally, as demonstrated in Ref. [26] and confirmed by the some tests made in the present study, the off-diagonal imaginary elements of the relaxation matrix play a role at elevated pressure. They do not significantly change the shape of the branches but manifest themselves through opposite spectral shifts of the P and R branches when the

line overlapping is very important. In order to take this effect into account, imaginary off-diagonal coupling terms within branches were added. They verify the detailed balance principal, have opposite signs for R-R and P-P couplings and decrease with the line separation. Their values were computed, for all bands at all pressures and temperatures, from a single parameter which was adjusted on a 72 atm spectrum of the  $(2\nu_1+\nu_3)_2$  band.

The previously mentioned inaccuracy of some line intensities in the former version of our data/software package [4] is illustrated by the results in Fig. 4, which are for the  $2\nu_1+\nu_3$  triad. In fact, as confirmed by recent high resolution studies [12], in HITRAN 2000, the intensity of the first band [ $(2\nu_1+\nu_3)_3$ , near  $4850\text{ cm}^{-1}$ ] was overestimated by about 10%, that of the second one [ $(2\nu_1+\nu_3)_2$  near  $4980\text{ cm}^{-1}$ ] being too high by about 4%, while that of the highest frequency one [ $(2\nu_1+\nu_3)_1$  near  $5100\text{ cm}^{-1}$ ] was correct. Note that the  $3\nu_1+\nu_3$  tetrad shows similar problems, the intensities of the R branches of the  $(3\nu_1+\nu_3)_2$  and  $(3\nu_1+\nu_3)_3$  bands being overestimated by about 5%, for instance. Note that the lowest curve in Fig. 4 is a first indication, further confirmed below, of the great improvement brought by updating our database.

Comparisons between measured spectra and those calculated using the updated version of our data/software package are presented below for various bands, pressures and temperature.

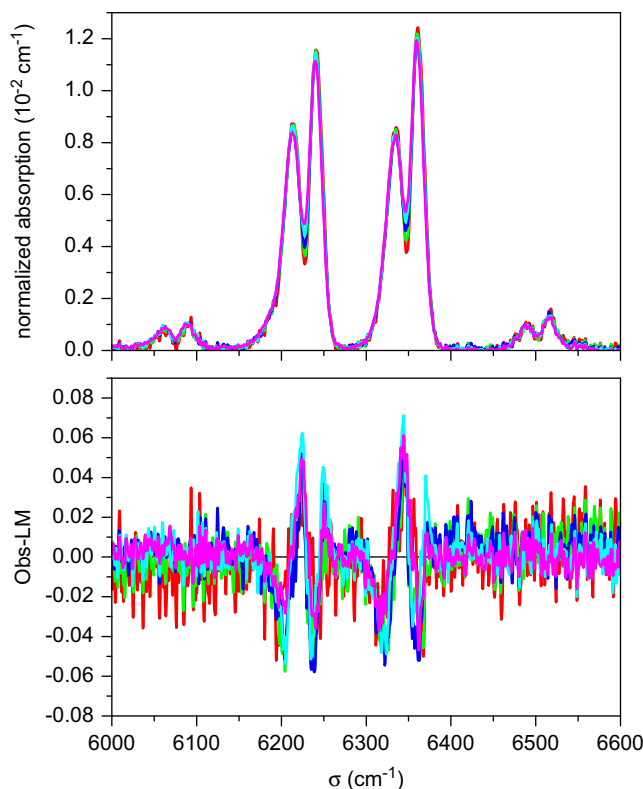


**Fig. 7.** Absorption coefficients and meas-calc residuals for 10%  $\text{CO}_2$  in five pressures (from 30 to 76.0 atm) of  $\text{N}_2$  at 295.15 K in the region of the  $(3\nu_1+\nu_3)$  tetrad. The top panel displays the measured absorptions normalized to unity area through integration over  $\sigma$ . The lower panel displays the residuals (meas-calc) obtained from calculations with our new database taking line-mixing into account.



A first result, obtained at room temperature in the  $(2\nu_1 + \nu_3)_2$  band, is plotted in Fig. 5. It shows that line-mixing has large effects at the studied pressures, as expected. This process leads, as is well known, to a narrowing of the branches and an enhancement of the peak absorptions (up to a 50% increase of the R branch for the highest pressure in Fig. 5). This plot also shows that our line-mixing model almost perfectly reproduces the measurements. This statement is confirmed by the results for the entire  $2\nu_1 + \nu_3$  triad plotted in Fig. 6. The measured-calculated deviations, which reach more than 30% of the peak values when line-mixing is neglected, typically remain within 2% when our model is used.

Similar comparisons, but for the  $3\nu_1 + \nu_3$  tetrad, are plotted in Fig. 7. The errors introduced by neglecting line-mixing being quantitatively similar to those in Figs. 5 and 6, the associated results are not displayed. Again, the agreement between measured and calculated values is good, although slightly less than in the triad. Note that most deviations are due to a slight frequency shift but that the calculated R branches are slightly too narrow leading to an overestimation of their peaks by about 3%.

The  $3\nu_3$  band, whose absorption was recorded together with those of the tetrad, is interesting from the point of view of line-mixing effects due to the particular structure of the R branch. Indeed, the R branch head occurs around

R(40) making this branch narrower and significantly more affected by line-mixing than most R branches of other  $\Sigma - \Sigma$  bands. Again, the robustness of our line-mixing model and the large errors obtained when this effect is neglected are demonstrated by Fig. 8.

Finally, the low-temperature results in Fig. 9 show that the effects of temperature are satisfactorily modeled in spite of a slightly poorer agreement with measured values than at room temperature (cf. Fig. 5), particularly in the trough between the R and P branches.

## 5. Conclusion

In the present study we propose an improved database/software package for the calculation of the  $\text{CO}_2$  absorption accounting for the line-mixing effects. The spectroscopic parameters were taken from the 2008 version of HITRAN and extended using the CDSD-296 and the high-temperature database CDSD-1000 when necessary. The improvement given by using the latest values for the spectroscopic parameters and the need to take line-mixing into account are clearly demonstrated using laboratory spectra recorded for various  $\text{CO}_2 + \text{N}_2$  mixtures and temperatures at elevated pressure. Moreover the very good agreement between calculated absorptions and those spectra for various bands shows the quality of the database proposed in this study.

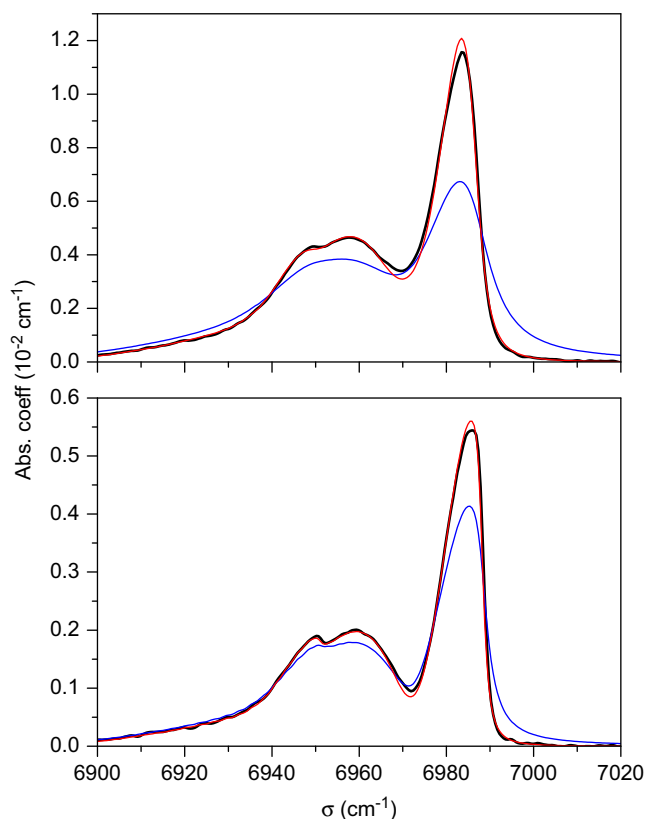


**Fig. 8.** Absorption coefficients for 10%  $\text{CO}_2$  in: 29.9 (bottom) and 72.3 atm (top) of  $\text{N}_2$  at 295.15 K in the region of the  $3\nu_3$  band. — are measured values, whereas — and — have been calculated with the new version of our database and software, respectively, neglecting line-mixing and taking this process into account.

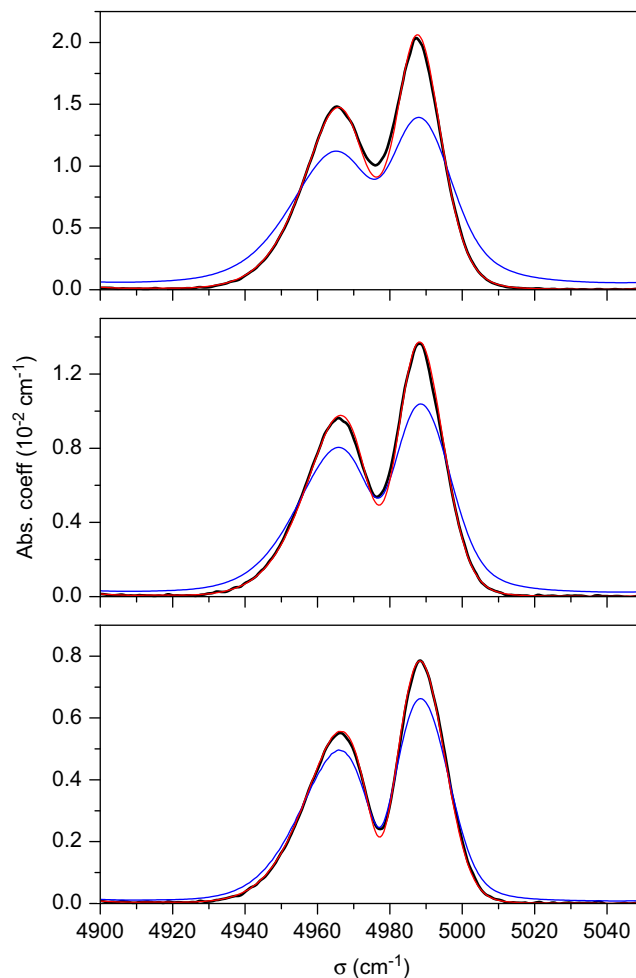


**Fig. 9.** Same as Fig. 5 but for a temperature of 218.2 K and total pressures, from bottom to top, of: 20.1, 35.6 and 54.0 atm.

The next step will consist of the application of this improved package to atmospheric spectra (recorded with various air masses, zenith angles, etc.) since all the changes described in this paper may enable a significant step toward the accuracy needed for the space-borne detection of CO<sub>2</sub> sinks and sources. Such an investigation in the 1.6–2.1  $\mu\text{m}$  region, similar to what was done in Ref. [6] but with a broader scope and the improved database, should confirm the quality of our data/software and yield more accurate retrievals. The question of longer wavelengths, and particularly the thermal domain near 13  $\mu\text{m}$ , has not been addressed in this paper. Nevertheless, for the intense bands in this region (e.g. the  $\nu_2$  and  $\nu_1 - \nu_2$  ones) the spectroscopic and line-mixing data have not changed since the former version of our database. The impact for retrievals is thus expected to be small (but this should be checked) and essentially due to the addition of weak transitions.

The new database and software may also be improved by the newest edition of the high-temperature CSDS database (currently in preparation) that will be a primary source of the new HITEMP database [27]. It is expected that the prediction of higher- $J$  energy levels will be even

more reliable than in the edition of CSDS-1000 used in this work. Also, after the inconsistencies in adoption of some experimentally measured pressure-induced parameters in HITRAN2008 are removed, the good experimental values will replace empirically determined values used in this work. This paper is a first and important step in bringing the HITRAN CO<sub>2</sub> data to the next generation of accuracy by supplying the consistent set of line-mixing parameters for all the bands of all isotopologues tabulated in the database.

The current software and database can be obtained from the corresponding author, and will be available in a future update of HITRAN.

### Acknowledgments

J. Lamouroux, A.L. Laraia, and R.R. Gamache are pleased to acknowledge support of this research by the National Science Foundation through Grant no. ATM-0803135. Any opinions, findings, and conclusions or recommendations expressed in this material are those of the author(s) and do not necessarily reflect the views of the National

Science Foundation. The authors from LISA acknowledge support by the TOSCA program of the Centre National d'Etudes Spatiales.

## Appendix A. Mass dependence of broadening coefficients

It is well known [1] that, assuming resonant collisions and a single intermolecular potential in  $R^{-q}$ , the temperature dependence coefficient of the broadening parameter  $\gamma$ , expressed in  $\text{cm}^{-1}/\text{molecule}$ , is

$$\gamma(T) \propto T^{(q-3)/2(q-1)}. \quad (\text{A1})$$

This law is quite well verified for  $\text{CO}_2$ -air, for instance. Indeed, the quadrupole–quadrupole interaction being dominant for this system, one has  $q=5$  and Eq. (A1) leads to  $T^{1/4}$ . This translates to  $T^{-1+1/4}$  when  $\gamma$  is in  $\text{cm}^{-1}/\text{atm}$ , corresponding to a temperature exponent of  $n=0.75$  in good agreement with the HITRAN value.

Recalling that the temperature dependence in Eq. (A1) essentially arises from the mean relative speed  $v_r(T)$  in intermolecular collisions, and since  $v_r(T)$  is proportional to  $\sqrt{T/\mu}$  one thus has

$$\gamma(T) \propto v_r(T)^{(q-3)/(q-1)}, \quad (\text{A2})$$

i.e.

$$\gamma(T) \propto \mu^{-(q-3)/2(q-1)}, \quad (\text{A3})$$

where  $\mu$  is the reduced mass. Hence, starting from the broadening of  $^{12}\text{C}^{16}\text{O}_2$  lines by collisions with partner X, the values for other isotopologues can be deduced from:

$$\left( \frac{\gamma(^{m1}\text{O}m2\text{C}m3\text{O}-X)}{\gamma(^{16}\text{O}^{12}\text{C}^{16}\text{O}-X)} \right) = \left( \frac{\mu(^{m1}\text{O}m2\text{C}m3\text{O}-X)}{\mu(^{16}\text{O}^{12}\text{C}^{16}\text{O}-X)} \right)^{-\alpha_X}, \quad (\text{A4})$$

where  $\mu(^{m1}\text{O}m2\text{C}m3\text{O}-X)$  is the reduced mass of the  $m1\text{O}m2\text{C}m3\text{O}-X$  collisional pair. For  $X=\text{H}_2\text{O}$  and air,  $\alpha_{\text{H}_2\text{O}}=1/6$  and  $\alpha_{\text{Air}}=1/4$ , respectively associated with the quadrupole–dipole ( $q=4$ ) and quadrupole–quadrupole ( $q=5$ ) interactions. Note that this assumes that the intermolecular potential is independent of the isotopologue.

## References

- [1] Hartmann JM, Boulet C, Robert D. Collisional effects on molecular spectra. Laboratory experiments and models, consequences for applications. Amsterdam: Elsevier; 2008.
- [2] Niro F, Boulet C, Hartmann JM. Spectra calculations in central and wing regions of  $\text{CO}_2$  IR bands between 10 and 20  $\mu\text{m}$ . I: model and laboratory measurements. J Quant Spectrosc Radiat Transfer 2004;88:483–98.
- [3] Niro F. Etudes théorique et expérimentale des profils collisionnels dans les centres et ailes des bandes infrarouges de  $\text{CO}_2$ . Applications à la simulation et à l'inversion de spectres atmosphériques. PhD thesis, Université d'Orsay, 2003.
- [4] Niro F, Jucks KW, Hartmann JM. Spectra calculations in central and wing regions of  $\text{CO}_2$  IR bands between 10 and 20  $\mu\text{m}$ . IV: software and database for the computation of atmospheric spectra. J Quant Spectrosc Radiat Transfer 2005;95:469–81.
- [5] Masiello G, Serio C, Carissimo A, Grieco G, Matricardi M. Application of  $\varphi$ -IASI to IASI: retrieval products evaluation and radiative transfer consistency. Atmos Chem Phys 2009;9:8771–83.
- [6] Hartmann JM, Tran H, Toon GC. Influence of line mixing on the retrievals of atmospheric  $\text{CO}_2$  from spectra in the 1.6 and 2.1  $\mu\text{m}$  regions. Atmos Chem Phys 2009;9:7303–12.

- [7] Rothman LS, Barbe A, Benner DC, Brown LR, Camy-Peyret C, Carleer MR, et al. The HITRAN molecular spectroscopic database: edition of 2000 including updates through 2001. J Quant Spectrosc Radiat Transfer 2003;82:5–44.
- [8] Ohshima H, Morino I, Nagahama T, Machida T, Suto H, Oguma H, et al. Column-averaged volume mixing ratio of  $\text{CO}_2$  measured with ground-based Fourier transform spectrometer at Tsukuba. J Geophys Res 2009;114:D18303, doi:10.1029/2008JD011465.
- [9] Crisp D, Atlas RM, Bréon FM, Brown LR, Burrows JP, Ciais P, et al. The Orbiting Carbon Observatory (OCO) mission. Adv Space Res 2004;34:700–9.
- [10] Kuze A, Kondo K, Kaneko Y, Hamazaki T. Greenhouse gases observation from the GOSAT satellite. AGU 2005 fall meeting abstracts, p. A14C-03.
- [11] Miller CE, Brown LR, Toth RA, Benner DC, Malathy Devi V. Spectroscopic challenges for high accuracy retrievals of atmospheric  $\text{CO}_2$  and the Orbiting Carbon Observatory (OCO) experiment. CR Phys Acad Sci Paris 2005;8:876–87.
- [12] Toth RA, Brown LR, Miller CE, Malathy Devi V, Benner DC. Spectroscopic database of  $\text{CO}_2$  line parameters: 4300–7000  $\text{cm}^{-1}$ . J Quant Spectrosc Radiat Transfer 2008;109:906–21.
- [13] Rothman LS, Gordon IE, Barbe A, Benner DC, Bernath PF, Birk M, et al. The HITRAN 2008 molecular spectroscopic database. J Quant Spectrosc Radiat Transfer 2009;110:533–72.
- [14] Hartmann JM. A simple empirical model for the collisional spectral shift of air-broadened  $\text{CO}_2$  lines. J Quant Spectrosc Radiat Transfer 2009;110:2019–26.
- [15] Sung K, Brown LR, Toth RA, Crawford TJ. Fourier transform infrared spectroscopy measurements of  $\text{H}_2\text{O}$ -broadened half-widths of  $\text{CO}_2$  at 4.3  $\mu\text{m}$ . Can J Phys 2009;87:469–84.
- [16] Rothman LS, Jacquemart D, Barbe A, Benner DC, Birk M, Brown LR, et al. The HITRAN 2004 molecular spectroscopic database. J Quant Spectrosc Radiat Transfer 2005;96:139–204.
- [17] Jucks KW, Rodrigues R, Le Doucen R, Claveaux C, Hartmann JM. Model, software, and database for computation of line-mixing effects in infrared Q branches of atmospheric  $\text{CO}_2$ . II. Minor and asymmetric isotopomers. J Quant Spectrosc Radiat Transfer 1999;63:31–48.
- [18] Rodrigues R, Jucks KW, Lacombe N, Blanquet G, Walrand J, Traub WA, et al. Model, software, and database for computation of line-mixing effects in infrared Q branches of atmospheric  $\text{CO}_2$ . I. Symmetric isotopomers. J Quant Spectrosc Radiat Transfer 1999;61:153–84.
- [19] Tashkun SA, Perevalov VI, Teffo JL. In: Agnès Perrin, Najate Ben Sari-Zizi, Jean Demaison, editors. CDS-296: the high-precision carbon dioxide spectroscopic databank: version for atmospheric applications, 161–169, 2006, in Remote Sensing of the Atmosphere for Environmental Security, Springer, Netherlands. (The 2008 updated version was used, available at: <ftp.iao.ru/pub/CDS-2008/296>).
- [20] Tashkun SA, Perevalov VI, Teffo JL, Bykov AD, Lavrentieva NN. CDS-1000, the high-temperature carbon dioxide spectroscopic databank. J Quant Spectrosc Radiat Transfer 2003;82:165–96 (The 2008 updated version was used, available at: <ftp.iao.ru/pub/CDS-2008/1000>).
- [21] Rothman LS, Hawkins RL, Wattson RB, Gamache RR. Energy levels, intensities, and linewidths of atmospheric carbon dioxide bands. J Quant Spectrosc Radiat Transfer 1992;48:537–66.
- [22] Tools to compute molecular densities for given temperature and pressure are available at <http://webbook.nist.gov/chemistry/form-ser.html>.
- [23] Thomas ME, Linevsky MJ. Integrated intensities of  $\text{N}_2$ ,  $\text{CO}_2$ , and  $\text{SF}_6$  vibrational bands from 1800 to 5000  $\text{cm}^{-1}$  as a function of density and temperature. J Quant Spectrosc Radiat Transfer 1989;42:465–76.
- [24] Maté B, Fraser GT, Lafferty WJ. Intensity of the simultaneous vibrational absorption  $\text{CO}_2$  ( $\nu_3=1$ )+ $\text{N}_2$  ( $\nu=1$ )+ $\text{CO}_2$  ( $\nu_3=0$ )+ $\text{N}_2$  ( $\nu=0$ ) at 4680  $\text{cm}^{-1}$ . J Mol Spectrosc 2000;201:175–7.
- [25] Tran H, Boulet C, Hartmann JM. Line-mixing and collision induced absorption by oxygen in the A-band. Laboratory measurements, model, and tools for atmospheric spectra computations. J Geophys Res 2006;D11:6869–82.
- [26] Rodrigues R, Hartmann JM, Bonamy L, Boulet C. Temperature, pressure, and perturber dependencies of line-mixing effects in  $\text{CO}_2$  infrared spectra. II. Angular momentum relaxation and spectral shift in  $\Sigma$ – $\Sigma$  bands. J Chem Phys 1998;109:3037–47.
- [27] Rothman LS, Gordon IE, Barber RJ, Dothe H, Gamache RR, Goldman A, Perevalov V, Tashkun SA, Tennyson J. HITEMP, the high-temperature molecular spectroscopic database. J Quant Spectrosc Radiat Transfer, submitted for publication.